Received: 29 September 2023 | Accepted: 13 May 2024

DOI: 10.1111/evj.14111

ORIGINAL ARTICLE

Equine Veterinary Journal WILEY

Auxiliary osseous findings in fetlocks of non-racing sports horses with sagittal groove disease of the proximal phalanx on low-field magnetic resonance imaging

Josephine E. Faulkner[1] | Zoë Joostens[2] | Bart J. G. Broeckx[3] | Stijn Hauspie[2] | Tom Mariën[2] | Katrien Vanderperren[1]

[1]Department of Morphology, Imaging, Orthopedics, Rehabilitation and Nutrition, Faculty of Veterinary Medicine, Ghent University, Merelbeke, Belgium

[2]Equine Diagnostic Centre, Equitom Equine Clinic, Lummen, Belgium

[3]Department of Veterinary and Biosciences, Faculty of Veterinary Medicine, Ghent University, Merelbeke, Belgium

Correspondence
Josephine E. Faulkner, Department of Morphology, Imaging, Orthopedics, Rehabilitation and Nutrition, Faculty of Veterinary Medicine, Ghent University, Salisburylaan 133, 9820 Merelbeke, Belgium.
Email: josie.faulkner@ugent.be

Abstract

Background: Sagittal groove disease of the proximal phalanx in equine athletes is commonly considered a bone stress injury. Repetitive hyperextension of the fetlock under high load is thought to contribute to its development. Concurrent changes are often reported in the dorsal sagittal ridge of the third metacarpus/metatarsus (MC3/MT3).

Objectives: To describe the spectrum of associated osseous abnormalities that are present in the fetlock in a large group of horses diagnosed with sagittal groove disease on low-field magnetic resonance imaging (MRI).

Study design: Retrospective, cross-sectional.

Methods: MRI images of horses diagnosed with sagittal groove disease at Equitom Equine Clinic between March 2014 and March 2023 were evaluated using semi-quantitative grading schemes and a sagittal groove disease MRI classification system.

Results: MRIs of 132 limbs were evaluated, predominantly from warmbloods used for showjumping ($n = 83$) and dressage ($n = 18$). Osseous densification and bone oedema-like signal grades were higher in the dorsal sagittal ridge than palmarly/plantarly ($p < 0.001$ and $p < 0.05$, respectively). Grades of both osseous densification and bone oedema-like signal in the dorsal sagittal ridge did not significantly differ between the different sagittal groove disease MRI classifications (both $p > 0.05$).

Main limitations: Inclusion based on original MRI reports, absence of control group, small numbers within some grading groups hindering statistical analyses.

Conclusions: Findings support the aetiological theories of chronic bone-stress due to loaded fetlock hyperextension however the severity of osseous changes of the dorsal sagittal ridge does not appear to be associated with the severity of sagittal groove disease classification.

KEYWORDS
bone oedema, fissure, horse, hyperextension, MRI, P1

1 | INTRODUCTION

Injury of the sagittal groove of the proximal phalanx (P1) is recognised in racehorses and sports horses taking part in other disciplines.[1–13] In the last 25 years the dominant aetiological theory for sagittal groove disease has been a maladaptive response to repetitive bone stress loading; a concept which is supported by diagnostic imaging, biomechanical and bone-mineral density studies.[2–6,9,11,12,14–18] It is thought that accelerated osseous modelling occurs at sites of cumulative microdamage in the sagittal groove with osteoclastic resorption leading to microfractures, and in some cases resulting in fissure/fracture formation.[12,18] A novel sagittal groove disease magnetic resonance imaging (MRI) classification system was recently published, based on a similar model to the Modified Fredericson MRI Classification System that is used in human medicine for tibial stress injuries and conceptually aiming to reflect the continuum of physiological and pathological changes which can occur in the sagittal groove (Table S1).[19–22]

Adaptive and maladaptive responses to repetitive bone stress may concurrently occur in other regions of the joint. For horses with sagittal groove disease, this is reported to occur most commonly at the distodorsal aspect of the sagittal ridge of the third metacarpus (MC3) or metatarsus (MT3), suggesting an association with hyperextension.[3,5,6,9] Biomechanical research supports the loaded extension theory and has also shown that the predominant biomechanical contributor to sagittal fracture of P1 is likely to be shear forces.[15–17,23]

MRI is a well-established modality for the assessment of bone stress injuries due to its ability to detect both osseous densification and bone oedema-like signal (bone oedema-like lesions).[3–6,12,24,25] To date there are no studies evaluating the distribution and severity of osseous findings in the rest of the fetlock joint in a large group of horses diagnosed with sagittal groove disease on MRI.

The aims of this study were therefore (1) to describe the range of osseous abnormalities in the distal aspect of MC3/MT3 and P1 associated with sagittal groove disease in a large group of horses at initial MRI examination, and (2) establish if the severity of sagittal groove disease was associated with severity of the changes in the dorsodistal aspect of MC3/MT3. It was hypothesised that (1) osseous densification and bone oedema-like signal would be increased in the dorsal aspect of the MC3/MT3 condyles compatible with an injury sustained during fetlock hyperextension, (2) higher grades of pathology in the dorsal aspect of the sagittal ridge of MC3/MT3 would be associated with higher sagittal groove disease classification.

2 | MATERIALS AND METHODS

2.1 | Case selection

The study was retrospective, descriptive and cross-sectional in design and no approval by an ethical committee was required. Horses included in the study were initially selected for another study that evaluated the spectrum of findings within the sagittal groove in horses with sagittal groove disease.[22] Briefly, criteria for inclusion were: horses of at least 1 year old which had low-field MRI of one or more fetlocks at Equitom Equine Clinic during the period March 2014 to March 2023 and in which abnormalities of the sagittal groove were identified. Dates were selected to ensure the largest possible convenience sample and reflected the life span of the MRI unit at this facility at the time of the study. Referrals came from within and external to the hospital. Cases were identified by search of archived MRI reports by one author (ECVDI certified radiologist, Radiologist 1) using the keywords 'P1', 'proximal phalanx', 'sagittal groove', 'sagittal groove disease', 'fissure' and 'incomplete fracture'. Clinical information as provided by the referring veterinarian was collected and anonymised by Radiologist 1. Clinical information collected included the date of MRI examination, signalment (birth date, sex, breed), clinical history (athletic use, level of work, reason for MRI, duration of lameness, previous imaging examinations) and clinical examination findings (lame limb, severity, localising clinical signs such as fetlock joint distension, response to flexion, results of local anaesthetic blocks). Cases were categorised into two groups: horses presented due to lameness and those without lameness in which a sagittal groove lesion was detected or suspected on screening radiographic examination (e.g., pre-purchase examination, osteochondrosis screening). Lameness status was determined on the basis of clinical history and clinical examination findings from referring veterinarians. A lameness examination was performed by the referring veterinarian but standardised method of determining lameness was not used.

Lame horses which underwent multi-limb MRI were assumed to have lameness in all examined limbs even if it was not explicitly stated in the clinical history. The original MRI reports were written predominantly by ECVDI-certified radiologists (2016–2023) with a small number written by an experienced and competent diagnostic imaging veterinarian (2014–2018). In cases with serial MRI examinations, only the first MRI examination in which a diagnosis of sagittal groove disease was made was included in the study.

2.2 | Magnetic resonance imaging examination protocol

All cases underwent standing MRI examination of the fetlock under sedation with an open 0.27 T permanent magnetic resonance system (Hallmarq EQ2) (Text S1). MRI studies were retrieved and anonymised by Radiologist 1.

2.3 | Magnetic resonance imaging evaluation

Images were retrospectively graded by an ECVDI-certified radiologist (Radiologist 2) who was blinded to the horse signalment and clinical history. Cases were evaluated using a DICOM viewer (Horos v.4.0.0 RC5, horosproject.org) in a random order (Random Sequence Generator: www.random.org/sequences). All available sequences were used for assessment and the observer followed the semi-quantitative grading schemes and sagittal groove disease

MRI classification system described below during image evaluation. If it was impossible to evaluate a criterium due to a lack of appropriate sequences or excessive artefact, this was noted as 'cannot evaluate'. Examinations with insufficient sequences for adequate assessment of the majority of criteria were excluded on agreement by Radiologists 1 and 2.

Once the image evaluation was complete, Radiologist 2 compared the grading data to the original MRI reports to check for conflicting findings. In the case of a discrepancy, the images were re-examined and the grade according to the grading scheme took precedence over the term used in the original report. These discrepancies were not recorded unless they concerned the presence or absence of lesions in the sagittal groove. In these cases, they were recorded and later evaluated by an EVCDI-certified radiologist (Radiologist 3) who made the deciding verdict (majority rule decision-making).

2.3.1 | Evaluation of the sagittal groove of the proximal phalanx

The sagittal groove of P1 was evaluated using a semi-quantitative grading scheme that evaluated subchondral defects, subchondral demineralisation, osseous densification and bone oedema-like signal in three subregions (dorsal, middle and palmar/plantar).[21,22] The data were used to classify the sagittal groove according to the sagittal groove disease MRI classification system, which reflects suspected pathways of pathological progression and severity of chronic overload/stress injury in this region (Table S1).[18–22] The overall sagittal groove disease MRI classification was assigned to the limb using the highest ranking from the three subregions. Briefly, the sagittal groove disease MRI classifications were: (0) normal, (1a) minor subchondral defect, (1b) microfissure (<3 mm proximodistal length), (2a) mild osseous densification, (2b) moderate to severe osseous densification, (3a) subchondral microfissure with mild osseous densification, (3b) subchondral microfissure with moderate to severe osseous densification, (4a) bone oedema-like signal within the subchondral ± trabecular bone, (4b) bone oedema-like signal with subchondral microfissure, (4c) bone oedema-like signal with subchondral demineralisation, (5) incomplete macrofissure/fracture and (6) complete fracture.

2.3.2 | Evaluation of the remainder of the proximal phalanx

The remainder of the proximal aspect of P1 was assessed using a semi-quantitative grading scheme (Table S2). Criteria were adapted from previous publications[24,25] and consideration was given to the reported ranges of subchondral bone thickness in P1 obtained from post-mortem specimens on microcomputed tomography.[14] The medial and lateral foveas/glenoids of P1 were evaluated as two independent regions for subchondral bone defects (grades 0–3), subchondral demineralisation/resorption (grades 0–3), osseous densification (grades 0–3) (Figure 1), bone oedema-like signal (grades 0–3) and osseous cyst-like lesion (OCLLs).

2.3.3 | Evaluation of the distal aspect of the third metacarpus/metatarsus

The sagittal ridge, medial and lateral condyles of the MC3/MT3 were assessed as separate entities and each was divided into two subregions (dorsal and palmar/plantar), giving six subregions.[24,25] Any parasagittal lesion located at the boundary between the sagittal ridge and medial or lateral condyle was recorded with the condyle rather than the sagittal ridge. Each subregion was evaluated for subchondral bone defects (grades 0–3), subchondral demineralisation/resorption (grades 0–3), osseous densification (grades 0–3) (Figure 2), bone oedema-like signal (grades 0–3) and OCLLs using a semi-quantitative grading scheme based on previous publications (Table S2).[24,25]

2.3.4 | Evaluation of the fetlock joint

The fetlock joint was graded for osteophytosis (grades 0–3), joint effusion (grades 0–3) and synovial proliferation (grades 0–3) using a semi-quantitative grading scheme based on previously published scales (Table S2).[24,25] Additionally, presence of dorsal fibrous articular capsule thickening was assessed.[26,27]

As the focus of the investigation was bone stress/fatigue injury of the sagittal groove it was elected not to evaluate other soft tissue

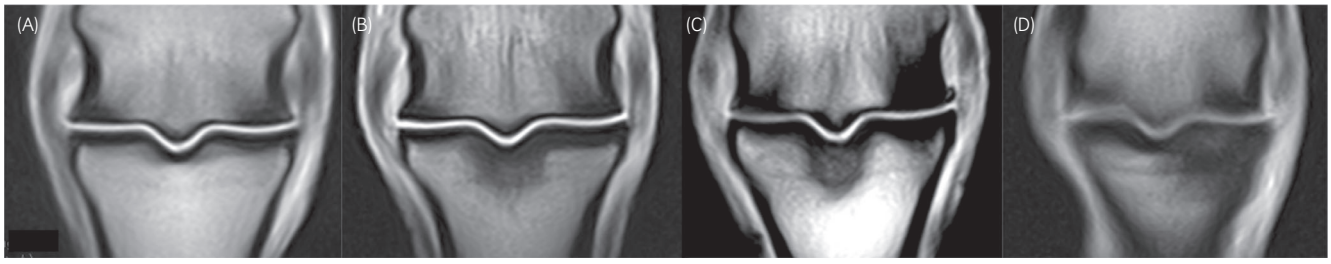

FIGURE 1 Frontal plane T1-weighted gradient recalled echo magnetic resonance images of fetlocks with different grades of osseous densification of the medial fovea of the proximal phalanx: (A) grade 0; (B) grade 1; (C) grade 2; (D) grade 3. Medial is located to the right of the image.

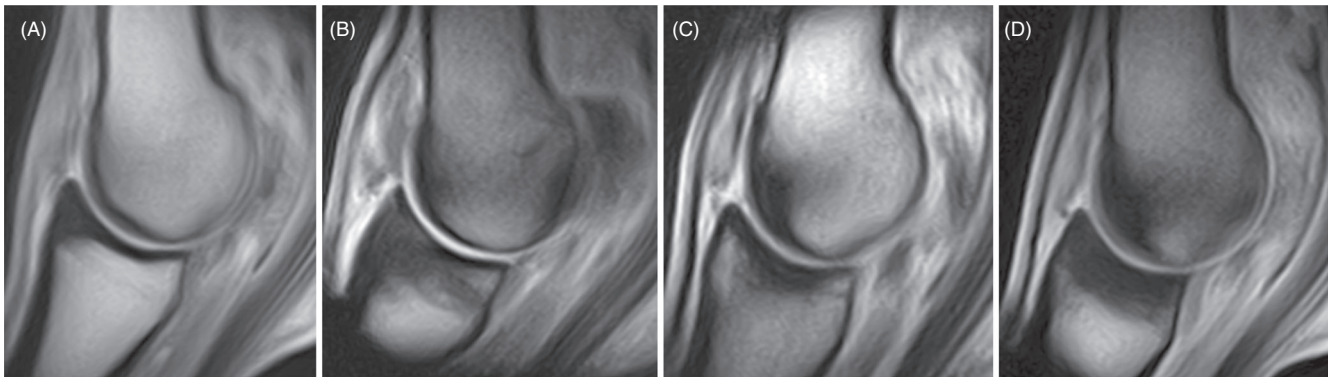

FIGURE 2 Sagittal plane T1-weighted gradient recalled echo magnetic resonance images of the fetlock in limbs with sagittal groove disease magnetic resonance imaging classification 5 (macrofissure) which show differing grades of osseous densification of the sagittal ridge: (A) dorsal grade 0, palmar grade 0; (B) dorsal grade 1, palmar grade 1; (C) dorsal grade 2, palmar grade 0; (D) dorsal grade 3, palmar grade 0.

lesions, osteochondral fragments or MRI findings in other regions (foot, pastern, MC3/MT3, carpus/tarsus). Cartilage signal was also not included in the assessment as this is not reliable when using a standing low-field magnetic resonance system.[28]

2.4 | Data analysis

Descriptive analysis was performed by J.F. using Microsoft Excel (Version 16.72, Microsoft Corporation). The statistical analysis was conducted by B.B. (R Version 4.2.2, R Foundation for Statistical Computing). Fisher exact test was used to evaluate the association between categorical variables in the MC3/MT3. This included the comparison of the semi-quantitative grading data between the dorsal and palmar/plantar aspects of each subregion of the MC3/MT3 and the comparison of sagittal groove disease classification with grades of osseous densification and bone oedema-like signal in the dorsal aspect of MC3/MT3. To correct for multiple testing, a Holm–Bonferroni correction was applied. Significance was set at $\alpha < 0.05$.

3 | RESULTS

3.1 | Horses

One hundred twelve horses were identified with sagittal groove disease. One horse was excluded from the study due to insufficient MRI sequences, resulting in the inclusion of 111 horses (55 mares, 9 stallions and 47 geldings) with mean ± SD age of 9.8 ± 3.1 years (range 1.3–18.5 years). Horse breeds included 104 warmbloods, 3 ponies, 2 Quarter Horses, 1 Arabian and 1 Friesian, and performance disciplines were 83 showjumping, 18 dressage, 5 leisure, 2 western, 1 eventing, 1 driving and 1 showing. Ninety-nine horses were lame and 12 horses were not lame. The amount of clinical information available varied markedly between horses and a summary of these additional findings is presented in Text S2.

3.2 | Magnetic resonance imaging acquisition

One horse that was diagnosed with bilateral forelimb sagittal groove disease had one limb that was excluded from the study due to insufficient sequences. Horses had either one ($n = 90$) or two limbs ($n = 21$) included in the study resulting in a total of 132 limbs evaluated: 44 left forelimb (LF), 59 right forelimb (RF), 17 left hindlimb (LH), 12 right hindlimb (RH). MRI sequences acquisition varied between cases (Text S1).

3.3 | Magnetic resonance imaging evaluation

There were 14 discrepancies between the grading of Radiologist 2 and the original report in terms of the identification of lesions in the sagittal groove. The results were altered accordingly following the second evaluation.

3.3.1 | Sagittal groove disease magnetic resonance imaging classification system

Overall sagittal groove disease MRI classifications were 1a (minor subchondral defect) in 2 limbs, 2a (mild osseous densification) in 27 limbs, 2b (moderate to severe osseous densification) in 1 limb, 3a (subchondral microfissure with mild osseous densification) in 7 limbs, 4a (bone oedema-like signal within the subchondral ± trabecular bone) in 36 limbs, 4b (bone oedema-like signal with subchondral microfissure) in 26 limbs, 4c (bone oedema-like signal with subchondral demineralisation) in 10 limbs and 5 (incomplete macrofissure/fracture) in 23 limbs.

3.3.2 | Semi-quantitative grading scheme

A summary of the semi-quantitative gradings for subchondral bone defects, subchondral demineralisation/resorption, osseous densification

TABLE 1 Semi-quantitative grading results for subchondral bone defects, subchondral demineralisation/resorption, osseous densification and bone oedema-like signal in the condyle of the third metacarpus/metatarsus in 132 limbs diagnosed with sagittal groove disease on MRI.

Region of MC3/MT3	Sub-region	SQ grade	Number of limbs (percentage)			
			Subchondral defects	Subchondral demineralisation	Osseous densification	Bone oedema-like signal
Sagittal ridge	D	0	109 (82.6)	130 (98.5)[a]	16 (12.1)[b]	66 (50)[c]
		1	22 (16.7)	1 (0.8)[a]	52 (39.4)[b]	42 (31.8)[c]
		2	1 (0.8)	1 (0.8)[a]	42 (31.8)[b]	22 (16.7)[c]
		3	0 (0)	0 (0)[a]	22 (16.7)[b]	2 (1.5)[c]
	P	0	124 (93.9)	132 (100)[a]	79 (59.8)[b]	125 (94.7)[c]
		1	8 (6.1)	0 (0)[a]	44 (33.3)[b]	6 (4.5)[c]
		2	0 (0)	0 (0)[a]	8 (6.1)[b]	1 (0.8)[c]
		3	0 (0)	0 (0)[a]	1 (0.8)[b]	0 (0)[c]
Medial condyle	DM	0	127 (96.2)[a]	129 (97.7)	29 (22)[b]	102 (77.3)[c]
		1	5 (3.8)[a]	2 (1.5)	55 (41.7)[b]	23 (17.4)
		2	0 (0)[a]	1 (0.8)	31 (23.5)[b]	7 (5.3)
		3	0 (0)[a]	0 (0)	17 (12.9)[b]	0 (0)
	PM	0	132 (100)[a]	128 (97)	59 (44.7)[b]	126 (95.5)
		1	0 (0)[a]	2 (1.5)	51 (38.6)[b]	2 (1.5)
		2	0 (0)[a]	1 (0.8)	18 (13.6)[b]	3 (2.3)
		3	0 (0)[a]	1 (0.8)	4 (3)[b]	1 (0.8)
Lateral condyle	DL	0	131 (99.2)	131 (99.2)[a]	110 (83.3)[b]	128 (97)
		1	1 (0.8)	1 (0.8)[a]	18 (13.6)[b]	4 (3)
		2	0 (0)	0 (0)[a]	3 (2.3)[b]	0 (0)
		3	0 (0)	0 (0)[a]	1 (0.8)[b]	0 (0)
	PL	0	131 (99.2)	132 (100)[a]	51 (38.6)[b]	127 (96.2)
		1	0 (0)	0 (0)[a]	68 (51.5)[b]	4 (3)
		2	1 (0.8)	0 (0)[a]	11 (8.3)[b]	0 (0)
		3	0 (0)	0 (0)[a]	2 (1.5)[b]	1 (0.8)

Note: Association between categorical variables in the dorsal and palmar/plantar aspects of each third metacarpus/metatarsus (MC3/MT3) subregion was evaluated with Fisher exact test with a Holm–Bonferroni correction.

Abbreviations: SQ, semi-quantitative; D, dorsal; P, palmar/plantar; DM, dorsomedial; PM, palmaro/plantaromedial; DL dorsolateral; PL, palmaro/plantarolateral.

[a]Not enough data present for at least one of the variables to perform the analysis.

[b]Statistically significant result $p < 0.001$.

[c]Statistically significant result $p < 0.05$.

and bone oedema-like signal in the condyle of MC3/MT3 is presented in Table 1. Osseous densification of the sagittal ridge had higher grading dorsally than palmarly/plantarly ($p < 0.001$). Grades of bone oedema-like signal of the sagittal ridge were higher dorsally compared with palmarly/plantarly ($p = 0.02$). There was a higher grading of osseous densification of the dorsal aspect of the medial condyle compared with palmarly/plantarly ($p < 0.001$). Osseous densification of the lateral condyle had lower gradings dorsally than palmarly/plantarly ($p < 0.001$). The remainder of comparisons either showed a lack of a statistically significant difference (subchondral defects in the sagittal ridge ($p = 1$) and lateral condyle ($p = 1$), subchondral demineralisation in the medial condyle ($p = 1$), bone oedema-like signal in the medial condyle ($p = 0.1$) and lateral condyle ($p = 1$)) or did not have enough grades present for one of the variables to perform the analysis (subchondral defects in the medial condyle, subchondral demineralisation in the sagittal ridge and lateral condyle).

Grades of osseous densification and bone oedema-like signal for the dorsal subregions of MC3/MT3 are shown alongside the corresponding sagittal groove disease MRI classification in Table 2. There was no significant difference in the sagittal groove disease MRI classification for the different grades of osseous densification for the dorsal aspect of the sagittal ridge ($p = 0.7$), medial condyle ($p = 0.6$) or lateral condyle ($p = 0.4$). Example images of differing grades of osseous densification of the sagittal ridge in limbs with sagittal groove disease MRI classification 5 (fissure) are shown in Figure 1. There was no significant difference in the sagittal groove disease MRI classification for the different grades of bone oedema-like signal for the dorsal aspect of the sagittal ridge ($p = 0.3$), medial condyle ($p = 0.9$) or lateral

TABLE 2 Semiquantitative grades of osseous densification and bone oedema-like signal in the dorsal subregions of the third metacarpus/metatarsus (MC3/MT3) relative to sagittal groove disease magnetic resonance imaging classification.

SQ grading criteria	Dorsal region of MC3/MT3	SQ grade	Number of limbs	MRI SGD classification											
				0	1a	1b	2a	2b	3a	3b	4a	4b	4c	5	6
Osseous densification	Sagittal ridge	0	16	0	1	0	6	0	0	0	3	3	0	3	0
		1	52	0	1	0	10	0	5	0	10	12	6	8	0
		2	42	0	0	0	8	1	1	0	15	7	2	8	0
		3	22	0	0	0	3	0	1	0	8	4	2	4	0
	Medial condyle	0	29	0	1	0	6	0	2	0	8	5	3	4	0
		1	55	0	1	0	9	1	3	0	10	16	3	12	0
		2	31	0	0	0	7	0	1	0	10	5	3	5	0
		3	17	0	0	0	5	0	1	0	8	0	1	2	0
	Lateral condyle	0	110	0	2	0	23	1	7	0	26	24	8	19	0
		1	18	0	0	0	2	0	0	0	8	2	2	4	0
		2	3	0	0	0	1	0	0	0	2	0	0	0	0
		3	1	0	0	0	1	0	0	0	0	0	0	0	0
Bone oedema-like signal	Sagittal ridge	0	66	0	2	0	18	1	5	0	14	14	4	8	0
		1	42	0	0	0	8	0	1	0	12	6	4	11	0
		2	22	0	0	0	1	0	1	0	9	6	1	4	0
		3	2	0	0	0	0	0	0	0	1	0	1	0	0
	Medial condyle	0	102	0	2	0	21	1	6	0	26	21	6	19	0
		1	23	0	0	0	5	0	0	0	7	5	3	3	0
		2	7	0	0	0	1	0	1	0	3	0	1	1	0
		3	0	0	0	0	0	0	0	0	0	0	0	0	0
	Lateral condyle	0	128	0	2	0	27	1	7	0	36	24	9	22	0
		1	4	0	0	0	0	0	0	0	0	2	1	1	0
		2	0	0	0	0	0	0	0	0	0	0	0	0	0
		3	0	0	0	0	0	0	0	0	0	0	0	0	0

Note: The association between semi-quantitative (SQ) grade and magnetic resonance (MRI) sagittal groove disease (SGD) classification was evaluated using Fisher exact test with a Holm–Bonferroni correction; no statistically significant differences were present.

TABLE 3 Semi-quantitative grading results for subchondral bone defects, subchondral demineralisation/resorption, osseous densification and bone oedema-like signal in the foveas of the proximal phalanx in 132 limbs diagnosed with sagittal groove disease on MRI.

Sub-region	SQ grade	Number of limbs (percentage)			
		Subchondral defects	Subchondral demineralisation	Osseous densification	Bone oedema-like signal
M	0	129 (97.7)	126 (95.5)	26 (19.7)	97 (73.5)
	1	3 (2.3)	4 (3)	91 (68.9)	30 (22.7)
	2	0 (0)	0 (0)	13 (9.8)	4 (3)
	3	0 (0)	2 (1.5)	2 (1.5)	1 (0.8)
L	0	131 (99.2)	132 (100)	75 (56.8)	126 (95.5)
	1	1 (0.8)	0 (0)	53 (40.2)	4 (3)
	2	0 (0)	0 (0)	3 (2.3)	2 (1.5)
	3	0 (0)	0 (0)	1 (0.8)	0 (0)

Abbreviations: L, lateral fovea; M, medial fovea; SQ, semi-quantitative.

condyle ($p = 0.07$). The remainder of the semi-quantitative grading results is shown alongside the corresponding sagittal groove disease MRI classifications in Table S3.

A summary of the semi-quantitative gradings for the foveas of P1 are shown in Table 3. One limb which had a small osseous cyst-like lesion (OCLL, $3 \times 4 \times 2$mm) located in the lateral parasagittal

subchondral bone of the sagittal groove also had two additional similarly sized small OCLLs in the medial fovea and palmarolateral MC3 condyle.

Osteophytosis was present to some degree in all fetlocks: grade 1 ($n = 72$), grade 2 ($n = 51$), grade 3 ($n = 9$). Synovial effusion grades were: grade 0 ($n = 3$), grade 1 ($n = 48$), grade 2 ($n = 56$), grade 3 ($n = 20$); and could not be evaluated in 5 limbs. Synovial proliferation grades were: grade 0 ($n = 22$), grade 1 ($n = 68$), grade 2 ($n = 33$), grade 3 ($n = 0$); and could not be evaluated in 9 limbs. Capsular thickening was present in 6 limbs and could not be evaluated in 1 limb. MRI grading results for the fetlock joint are shown in Table S3 alongside the corresponding sagittal groove disease MRI classifications.

4 | DISCUSSION

In this group of horses diagnosed with sagittal groove disease on MRI there was a high prevalence of abnormalities in the dorsal aspect of the sagittal ridge of MC3/MT3. In this region, almost 50% of limbs had grade 2–3 osseous densification and about 40% were grade 1. Additionally, almost 20% of limbs had bone oedema-like signal in the dorsal aspect of the sagittal ridge that was graded as 2–3 and over 30% were graded 1. Furthermore, it was shown that osseous densification and bone oedema-like signal had higher grades at the dorsal aspect of the sagittal ridge than the palmar/plantar aspect ($p < 0.001$ and $p > 0.05$, respectively). These findings are supportive of osseous modelling and injury sustained during loading in fetlock hyperextension. Nevertheless, these findings should be interpreted with a degree of caution as it has been reported in sound horses that the dorsal aspect of the subchondral bone plate of the sagittal ridge is thicker than the mid-distal and palmar/plantar aspects, with the range of thickness reported to be between 1 and 7 mm.[29] Additionally, the prevalence of osseous changes in the dorsal and palmar aspects of the sagittal ridge of MC3 have been shown to differ between Standardbred and Thoroughbred racehorses and therefore these may differ for the sport horse disciplines included in this study.[25] Similarly, caution must be used in interpreting the clinical significance of bone oedema-like lesions in the condyles of the MC3/MT3 in sports and pleasure horses as the severity of bone marrow lesions was shown not to be significantly associated with lameness nor with the type or level of activity that horses take part in.[30] In the present study, there was no significant difference in the dorsal sagittal ridge grades between sagittal groove disease MRI classifications. A group of control horses with sagittal groove disease MRI classification 0 would ideally be used to determine whether the dorsal densification and bone oedema-like signal is significantly more prevalent in horses with sagittal groove disease compared with horses without sagittal groove disease; however, none were present in the sample, as expected due to the inclusion criteria.

In the sports horses included in this study, densification was more common and had higher grades in the dorsal aspect of the medial condyle of MC3/MT3 compared with the palmar/plantar aspect ($p < 0.001$). This is similar to Standardbred racehorses presenting for MRI with injury of the fetlock, and differs from Thoroughbred racehorses where the extent of subchondral densification was higher palmarly.[25] Conversely, there was higher densification in the palmar/plantar half of the lateral condyle, compared with the dorsal half ($p < 0.001$). This is in agreement with the findings in both Standardbreds and Thoroughbreds.[25] These densification patterns are likely to reflect the forces sustained during exercise in different disciplines.

Grades of subchondral defects, demineralisation, osseous densification and bone oedema-like signal were all higher in the medial fovea of P1 than lateral, although defects and demineralisations were rather infrequent. This is consistent with the findings of an in vitro pressure distribution study which showed that pressure at the medial aspect of P1 is significantly higher than lateral during simulated walk[17] and an anatomical study that used microcomputed tomography to establish that the subchondral bone of the medial fovea was significantly thicker than the lateral in the middle and palmar aspects in both unraced and race-fit Thoroughbreds.[14]

The biomechanics of the fetlock joint have been evaluated in several in vitro studies using either warmblood or Thoroughbred cadaver limbs and in which the forces applied to the limbs result in the loads expected during particular gaits or actions. It has been shown that external axial rotation of P1 and collateromotion of the fetlock joint increase with increasing fetlock extension and that there is shear strain across the proximal aspect of P1.[15,23] As loads mimicking a gallop are approached (near maximal fetlock extension), there is a rapid increase in dorsoproximal P1 bone strain and a 30°–40° change in principal strain direction which is postulated to help to explain the mechanism of sagittal fractures of the equine proximal phalanx.[15,23] It is likely these forces contribute to osseous modelling at all stages of sagittal groove disease, not just at the time of fissuring. Given that a large proportion of the horses in this study were showjumpers, it should be noted that the loading expected in the fetlock during jumping (12 000 N) exceeds that of galloping (10 500 N).[16] Additionally, the biomechanical effects of turning have not yet been fully investigated, and this is likely to affect the forces between the sagittal ridge of the third metacarpal bone and the sagittal groove of the proximal phalanx in sport horses such as showjumpers and dressage horses.[6]

Cartilage was not assessed in this study due to the inherent limitations of low-field MRI however osteophytosis, subchondral sclerosis, lysis and synovial effusion have all been shown to be associated with the degree of cartilage damage.[24] Osteophytosis was present to some degree in all fetlocks, with 45% graded as moderate or severe (grade 3 or 4). It has been suggested that the presence of osteoarthritis may contribute to poor outcomes in cases of sagittal groove disease and therefore the severity of degenerative changes may be important when formulating prognoses.[3] Synovial effusion and proliferation grades were variable (ranging from 0 to 3 and 0 to 2, respectively). Joint capsule thickening is also a feature of osteoarthritis and was infrequently identified in this sample population. A previous study showed capsular inflammation and fibrosis were more severe in pathological fetlocks of Standardbreds than Thoroughbreds and a component of this is likely to be breed- or discipline-related.[25]

This research focused on osseous changes and soft tissues were not evaluated; however, this could be considered for further

investigation. Hyperextension of the fetlock can be a clinical symptom associated with desmopathy of the suspensory ligament and it would be interesting to undertake an investigation into whether there are any associations between pathology in the suspensory ligament and sagittal groove disease.[31,32]

Limitations of the study include that case selection was based on original MRI diagnoses, introducing bias and possibly underrepresenting some classifications of sagittal groove disease. Most horses used in this study were warmbloods used for showjumping and dressage and no racehorses were included in the sample, which reflects the clinical caseload. However, since analogous changes in the sagittal groove have been described in Thoroughbred and Standardbred racehorses, there are likely to be transferable findings between the disciplines and the extent to which this is true warrants further investigation. For most image evaluation criteria, only one observer graded the images followed by cross-checking with reports. Intra- and inter-observer variability of similar semi-quantitative grading schemes has been performed previously but should be repeated with these versions and the sagittal groove disease MRI classification system for validation.[24] Grading of images was challenging in some cases with lower image quality, especially those with movement artefact; however, this does reflect the reality of clinical practice. Small sample sizes in some groups precluded certain statistical analyses.

To conclude, the results support the biomechanical roles of repetitive bone stress injury and loaded fetlock hyperextension in the development of sagittal groove disease however the severity of sagittal groove disease does not appear to be correlated with the severity of changes in the dorsal aspect of the MC3/MT3. Further research should be done to establish whether the dorsal changes in MC3/MT3 are more pronounced in horses with sagittal groove disease than in those without.

FUNDING INFORMATION

None.

CONFLICT OF INTEREST STATEMENT

The authors declare no conflicts of interest.

AUTHOR CONTRIBUTIONS

Josephine E. Faulkner: Conceptualization; data curation; formal analysis; investigation; methodology; project administration; resources; validation; visualization; writing – original draft; writing – review and editing. **Zoë Joostens:** Conceptualization; data curation; investigation; methodology; project administration; resources; software; supervision; validation; writing – review and editing. **Bart J. G. Broeckx:** Data curation; formal analysis; resources; software; supervision; validation; writing – review and editing. **Stijn Hauspie:** Data curation; investigation; resources; supervision; validation; writing – review and editing. **Tom Mariën:** Conceptualization; project administration; resources; software; validation; writing – review and editing. **Katrien Vanderperren:** Conceptualization; investigation; methodology; project administration; resources; supervision; validation; writing – review and editing.

DATA INTEGRITY STATEMENT

J. Faulkner had full access to all the data in the study and takes responsibility for the integrity of the data and the accuracy of the data analysis.

ETHICAL ANIMAL RESEARCH

Research ethics committee oversight not required by this journal: retrospective study of clinical records.

INFORMED CONSENT

Explicit owner consent for animals' inclusion in the study was not stated.

PEER REVIEW

The peer review history for this article is available at https://www.webofscience.com/api/gateway/wos/peer-review/10.1111/evj.14111.

DATA AVAILABILITY STATEMENT

The data that support the findings of this study are available from the corresponding author upon reasonable request: Open sharing exemption granted by editor for this descriptive retrospective clinical report.

ORCID

Josephine E. Faulkner https://orcid.org/0000-0003-2597-4007
Zoë Joostens https://orcid.org/0000-0003-0116-4499
Bart J. G. Broeckx https://orcid.org/0000-0001-6742-3911
Katrien Vanderperren https://orcid.org/0000-0002-6375-5369

REFERENCES

1. Kuemmerle JM, Auer JA, Rademacher N, Lischer CJ, Bettschart-Wolfensberger R, Fürst AE. Short incomplete sagittal fractures of the proximal phalanx in ten horses not used for racing. Vet Surg. 2008;37(2):193–200. https://doi.org/10.1111/j.1532-950X.2007.00359.x
2. Brünisholz HP, Hagen R, Fürst AE, Kuemmerle JM. Radiographic and computed tomographic configuration of incomplete proximal fractures of the proximal phalanx in horses not used for racing. Vet Surg. 2015;44(7):809–15. https://doi.org/10.1111/vsu.12364
3. Gold SJ, Werpy NM, Gutierrez-Nibeyro SD. Injuries of the sagittal groove of the proximal phalanx in warmblood horses detected with low-field magnetic resonance imaging: 19 cases (2007–2016). Vet Radiol Ultrasound. 2017;58(3):344–53. https://doi.org/10.1111/vru.12488
4. Mizobe F, Nomura M, Ueno T, Yamada K. Bone marrow oedema-type signal in the proximal phalanx of Thoroughbred racehorses. J Vet Med Sci. 2019;81(4):593–7. https://doi.org/10.1292/jvms.18-0530
5. Lipreri G, Bladon BM, Giorio ME, Singer ER. Conservative versus surgical treatment of 21 sports horses with osseous trauma in the proximal phalangeal sagittal groove diagnosed by low-field MRI. Vet Surg. 2018;47(7):908–15. https://doi.org/10.1111/vsu.12936
6. Dyson S, Nagy A, Murray R. Clinical and diagnostic imaging findings in horses with subchondral bone trauma of the sagittal groove of the proximal phalanx. Vet Radiol Ultrasound. 2011;52(6):596–604. https://doi.org/10.1111/j.1740-8261.2011.01852.x
7. Curtiss AL, Ortved KF, Dallap-Schaer B, Gouzeev S, Stefanovski D, Richardson DW, et al. Validation of standing cone beam computed tomography for diagnosing subchondral fetlock pathology in the Thoroughbred racehorse. Equine Vet J. 2021;53(3):510–23. https://doi.org/10.1111/evj.13414

8. Smith MRW, Wright IM. Radiographic configuration and healing of 121 fractures of the proximal phalanx in 120 Thoroughbred racehorses (2007-2011). Equine Vet J. 2014;46(1):81–7. https://doi.org/10.1111/evj.12094
9. Powell S. Low-field standing magnetic resonance imaging findings of the metacarpo/metatarsophalangeal joint of racing Thoroughbreds with lameness localised to the region: a retrospective study of 131 horses. Equine Vet J. 2012;44(2):169–77. https://doi.org/10.1111/j.2042-3306.2011.00389.x
10. Markel MD, Richardson DW. Noncomminuted fractures of the proximal phalanx in 69 horses. J Am Vet Med Assoc. 1985;186(6):573–9.
11. Smith MRW, Wright IM. Are there radiologically identifiable prodromal changes in Thoroughbred racehorses with parasagittal fractures of the proximal phalanx? Equine Vet J. 2014;46(1):88–91. https://doi.org/10.1111/evj.12093
12. Ramzan PHL, Powell SE. Clinical and imaging features of suspected prodromal fracture of the proximal phalanx in three Thoroughbred racehorses. Equine Vet J. 2010;42(2):164–9. https://doi.org/10.2746/042516409X478695
13. Holcombe S, Schneider R, Bramlage L, Gabel A, Bertone A, Beard W. Lag screw fixation of noncomminuted sagittal fractures of the proximal phalanx in racehorses: 59 cases (1973-1991). J Am Vet Med Assoc. 1995;206(8):1195–9.
14. Noble P, Singer ER, Jeffery NS. Does subchondral bone of the equine proximal phalanx adapt to race training? J Anat. 2016;229(1):104–13. https://doi.org/10.1111/joa.12478
15. Singer E, Garcia T, Stover S. How does bone strain vary between the third metacarpal and the proximal phalangeal bones of the equine distal limb? J Biomech. 2021;123:110455. https://doi.org/10.1016/j.jbiomech.2021.110455
16. Brama PAJ, Karssenberg D, Barneveld A, van Weeren PR. Contact areas and pressure distribution on the proximal articular surface of the proximal phalanx under sagittal plane loading. Equine Vet J. 2001;33(1):26–32. https://doi.org/10.2746/042516401776767377
17. den Hartog SM, Back W, Brommer H, van Weeren PR. In vitro evaluation of metacarpophalangeal joint loading during simulated walk. Equine Vet J. 2009;41(3):214–7. https://doi.org/10.2746/042516409X395570
18. Lin ST, Foote AK, Bolas NM, Peter VG, Pokora R, Patrick H, et al. Three-dimensional imaging and histopathological features of third metacarpal/tarsal parasagittal groove and proximal phalanx sagittal groove fissures in Thoroughbred horses. Animals. 2023;13(18):2912. https://doi.org/10.3390/ani13182912
19. Fredericson M, Bergman AG, Hoffman KL, Dillingham MS. Tibial stress reaction in runners correlation of clinical symptoms and scintigraphy with a new magnetic resonance imaging grading system. Am J Sports Med. 1995;23(4):472–81.
20. Kijowski R, Choi J, Shinki K, Del Rio AM, De Smet A. Validation of MRI classification system for tibial stress injuries. Am J Roentgenol. 2012;198(4):878–84. https://doi.org/10.2214/AJR.11.6826
21. Faulkner JE, Joostens Z, Broeckx BJG, Hauspie S, Mariën T, Vanderperren K. Follow-up magnetic resonance imaging of sagittal groove disease of the equine proximal phalanx using a classification system in 29 non-racing sports horses. Animals. 2023;14(1):34. https://doi.org/10.3390/ani14010034
22. Faulkner JE, Joostens Z, Broeckx BJG, Hauspie S, Mariën T, Vanderperren K. Low-field magnetic resonance imaging of sagittal groove disease of the proximal phalanx in non-racing sport horses. Equine Vet J. 2024. Epub ahead of print. https://doi.org/10.1111/evj.14088
23. Singer E, Garcia T, Stover S. How do metacarpophalangeal joint extension, collateromotion and axial rotation influence dorsal surface strains of the equine proximal phalanx at different loads in vitro? J Biomech. 2013;46(4):738–44. https://doi.org/10.1016/j.jbiomech.2012.11.028
24. Olive J, D'anjou MA, Alexander K, Laverty S, Theoret C. Comparison of magnetic resonance imaging, computed tomography, and radiography for assessment of noncartilaginous changes in equine metacarpophalangeal osteoarthritis. Vet Radiol Ultrasound. 2010;51(3):267–79. https://doi.org/10.1111/j.1740-8261.2009.01653.x
25. Olive J, Serraud N, Vila T, Germain JP. Metacarpophalangeal joint injury patterns on magnetic resonance imaging: a comparison in racing Standardbreds and Thoroughbreds. Vet Radiol Ultrasound. 2017;58(5):588–97. https://doi.org/10.1111/vru.12512
26. Guerri G, Palozzo A, Straticò P, Varasano V, Celani G, Di Francesco P, et al. 2D-SWE of the metacarpophalangeal joint capsule in horses. Vet Sci. 2022;9(9):1–12. https://doi.org/10.3390/vetsci9090478
27. Denoix JM, Jacot S, Bousseau B, Perrot P. Ultrasonographic anatomy of the dorsal and abaxial aspects of the equine fetlock. Equine Vet J. 1996;28(1):54–62. https://doi.org/10.1111/j.2042-3306.1996.tb01590.x
28. Smith MA, Dyson SJ, Murray RC. Reliability of high- and low-field magnetic resonance imaging systems for detection of cartilage and bone lesions in the equine cadaver fetlock. Equine Vet J. 2012;44(6):684–91. https://doi.org/10.1111/j.2042-3306.2012.00561.x
29. Smith MA, Dyson SJ. Normal MRI anatomy: the fetlock region. In: Murray R, editor. Equine MRI. Chichester, UK: John Wiley & Sons, Ltd; 2011. p. 173–89. https://doi.org/10.1002/9781118786574.ch6
30. De Guio C, Ségard-Weisse E, Thomas-Cancian A, Schramme M. Bone marrow lesions of the distal condyles of the third metacarpal bone are common and not always related to lameness in sports and pleasure horses. Vet Radiol Ultrasound. 2019;60(2):167–75. https://doi.org/10.1111/vru.12700
31. Dyson SJ, Arthur RM, Palmer SE, Richardson D. Suspensory ligament desmitis. Vet Clin North Am Equine Pract. 1995;11(2):177–215. https://doi.org/10.1016/S0749-0739(17)30319-X
32. Marneris D, Dyson SJ. Clinical features, diagnostic imaging findings and concurrent injuries in 71 sports horses with suspensory branch injuries. Equine Vet Educ. 2014;26(6):312–21. https://doi.org/10.1111/eve.12175

SUPPORTING INFORMATION

Additional supporting information can be found online in the Supporting Information section at the end of this article.

How to cite this article: Faulkner JE, Joostens Z, Broeckx BJG, Hauspie S, Mariën T, Vanderperren K. Auxiliary osseous findings in fetlocks of non-racing sports horses with sagittal groove disease of the proximal phalanx on low-field magnetic resonance imaging. Equine Vet J. 2024. https://doi.org/10.1111/evj.14111